Response of the Equatorial Ionosphere over the South American Sector to the 2 - 6 February 2022 storm

Amadi B. C [1, 2], Eurico R. P [1], Liying Q [2], Angela S [1], Kherani E. A [1], Inez S.B [1], Denny O [3]

National Institute for Space Research (INPE), Brazil [1], National Center for Atmospheric Research (NCAR), Boulder [2], NASA Goddard SFC [3]

Abstract

With Nmax data from GOLD, GPS TEC, and neutral gas density from the MSIS model, we studied the development of irregularities in the equatorial ionosphere during the storm of 2 - 6 February 2022 by computing the ion-neutral gas collision frequency, local Hall and Pedersen conductivity. A comparison of results showed that high values of Hall conductivity and ion-neutral collision frequency may have suppressed the development of Equatorial Plasma Bubbles (EPB) observed on peak electron density map. This is likely due to the antagonistic behavior between collision frequency and the Rayleigh-Taylor Instability (RTI) growth rate required for EPB development. We also observed a relatively high local Hall conductivity on Days 03 and 04 associated with the non-occurrence of EPB.

Introduction

Energy flow into the ionosphere via the magnetosphere can be intensified during magnetic storms, and manifest as electric field ($\vec{E}$) and Joule heating as shown in Figure 1.

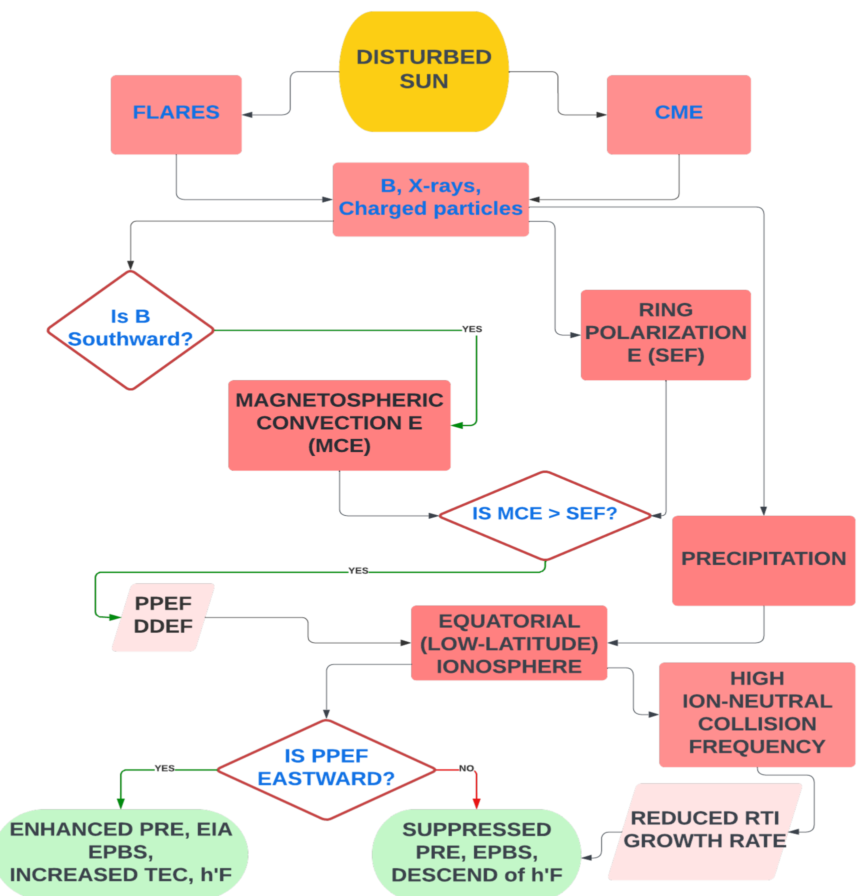

Figure 1. Flow of energy from the interplanetary medium into the equatorial ionosphere via the magnetosphere.

This $\vec{E}$ can penetrate the equatorial ionosphere and influence (enhance or inhibit) the growth rate of Rayleigh-Taylor instability (RTI) associated with the development of plasma irregularities such as Equatorial Plasma Bubbles (EPBs) (Eurico et al., 2019).

RTI is enhanced by the Eastward $\vec{E}$ but suppressed by high collision frequency and storms can drive either of these as illustrated above.

Motivation and Objectives

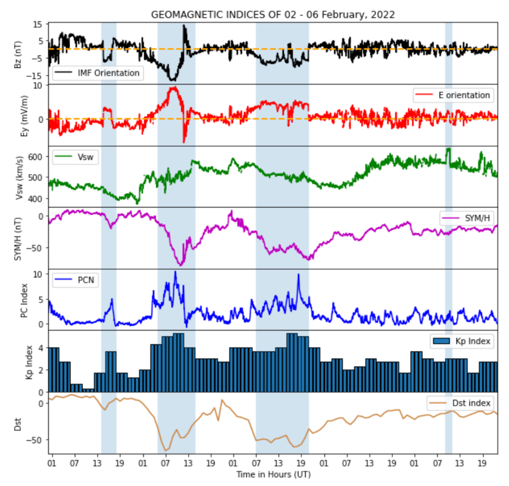

Figure 2. Features of the Geomagnetic storm of 2-6 February. Bz, Ey and Vsw are the North-South IMF component, East-West electric field and solar wind speed respectively.

On the 4th of February, 2022, a flare-induced Corona Mass Ejection (CME) caused a geomagnetic storm whose features are shown on Figure 2. Probably, this contributed to 40 starlink satellites that burnt on this storm day.

This event is likely associated with a significant increase in thermospheric neutral gas density (private discussion with Dr. Denny Oliveira, NASA) and catalysed changes in the thermosphere-ionosphere system (TIS) such as enhanced collision frequencies and consequent effects of satellite orbital drag (Oliveira and Zesta, 2019).

One of CEDAR's 2021 grand challenge is the understanding of storm-time TIS. **Thus, we aim to study for the first time, this new moderate but scientifically significant storm and some questions we sought to answer include:**

- **What is the variation in ion-neutral collision and its influence on the development of EPBs over the South American equatorial sector?**
- **How did the local conductivity vary during the period of this storm and what's its consequent effect on EPBs?**
- **Was the effect of ion-neutral collision and local conductivity in consonance or antagonistic?**

Methodology

The methodology used to attain our result is summarised in Figure 3.

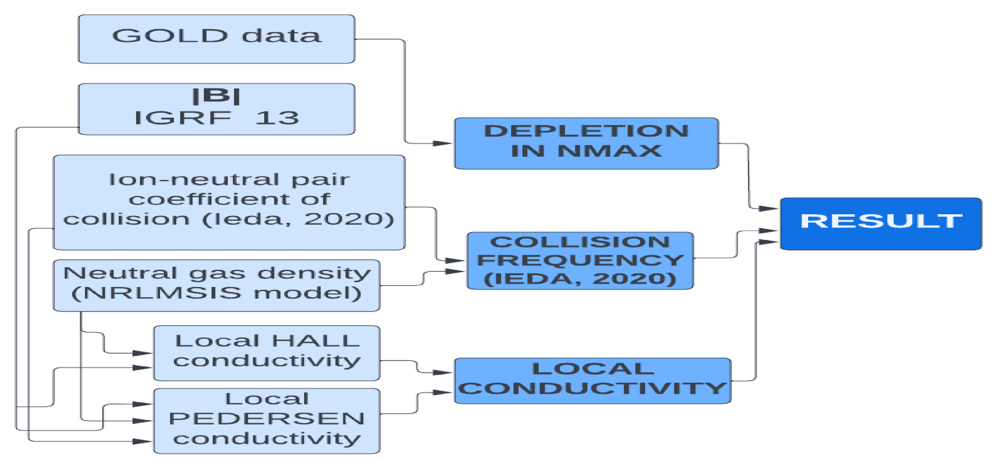

Figure 3. A flowchart of scientific methodology

For emphasis, the local Hall and Pedersen Conductivity are given as:

$$\sigma_P = \Sigma_i \frac{n_i e}{B} \frac{k_i}{1 + k_i^2} + \frac{n_e e}{B} \frac{k_e}{1 + k_e^2} \tag{1}$$

$$\sigma_H = -\Sigma_i \frac{n_i e}{B} \frac{k_i^2}{1 + k_i^2} + \frac{n_e e}{B} \frac{k_e^2}{1 + k_e^2} \tag{2}$$

Recall that $k = \frac{\Omega}{\nu}$ and $\Omega = \frac{eB}{m}$.
Considering the masses of ions (massive) and electrons, we can make the following approximations:

$$k_i \approx 0 \text{ and } k_e^2 \gg 1 \implies k_e^2 + 1 \approx k_e^2 \tag{3}$$

Thus, equations 1 and 2 reduces to:

$$\sigma_P = \frac{n_e e}{B} \frac{k_e}{1 + k_e^2} \text{ and } \sigma_H = \frac{n_e e}{B} \frac{k_e^2}{1 + k_e^2} \tag{4}$$

where n_i and n_e, B, k_i and k_e, Ω, ν, e and m represent the ion and electron density, magnitude of magnetic field, ion and electron mobility, gyrofrequency, collision frequency, electron charge and mass. The indices i and e are used to represent ion and electron respectively.

Equation 4 is the approximate local Pedersen and Hall conductivity from which the effect of their complementary $\vec{E}$ can be possibly inferred.

Result and Discussion

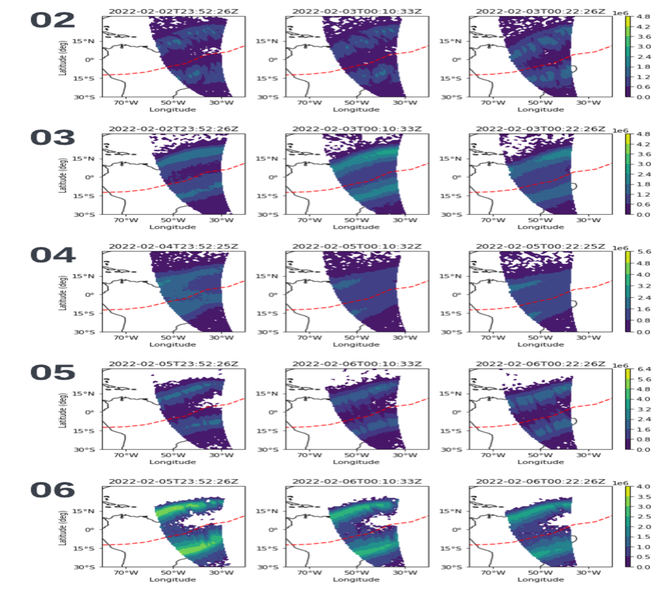

Figure 4. Peak electron density for Days 02 - 06 Feb, 2022. On days 03 and 04, EPB development was suppressed unlike days 02, 05 and 06.

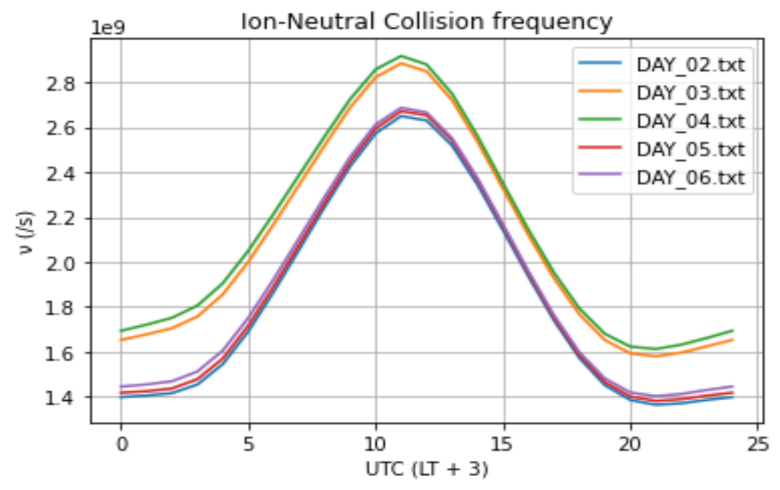

Figure 5. Daily variation in ion-neutral collision from 02 - 06 Feb, 2022 as computed from the Ieda (2020) model. Collision frequency was highest on Days 03 and 04.

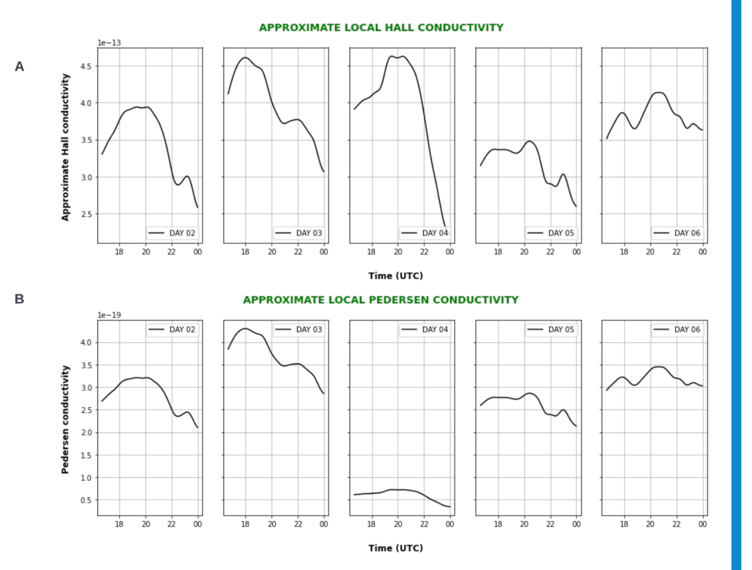

Figure 6. Approximate Hall and Pedersen Conductivity for Days 02 - 06. Hall conductivity was high on Days 03 and 04 and Pedersen conductivity was high on Day 03 and 06.

RESULT

1. Figure 4 shows the development of irregularities and Equatorial plasma bubbles (EPBs) on Days 02, 05 and 06 but not on Days 03 and 04, and
2. Figure 5 illustrates the temporal variation in ion-neutral collision frequency (ν_{in}) with high values obtained for Days 03 and 04 (orange and green plots respectively).
3. Interestingly, high values of local Hall conductivity were recorded on Days 03 and 04 as shown in Figure 6.

DISCUSSION

1. EPB development depends on upward $\vec{E} \times \vec{B}$ mechanism and RTI growth rate (γ), and Yokohama (2017) showed the dependence of γ on ν_{in} as follows:

$$\gamma = \frac{g}{\nu_{in}} \frac{1}{N} \frac{\partial N}{\partial z} \tag{5}$$

   This implies that the high ν_{in} observed on Days 03 and 04 suppressed γ and in turn EPB development on same days.

2. Additionally, ν_{in} reduces mobility and in turn σ_P, leading to a decrease in polarization and fringe $\vec{E}$ required for upward $\vec{E} \times \vec{B}$.

3. Thus, the non-occurrence of EPBs in the evening time ionosphere on Days 03 and 04 is very likely associated with the high ion-neutral collision frequency (ν_{in}) that occurred on same days as shown in Figure 5, and possibly acting in consonance with DDEF penetration to the equatorial ionosphere due to persistent southward turning of Bz as shown in Figure 2 (see Bz and PC index).

Conclusion

An important response of the equatorial ionosphere to geomagnetic and quiet time variations, is the evolution of EPBs that interfere navigational signal propagation. In an effort to improve prediction of EPB occurrence, we have carried out a comparative study that shows the following:

1. High ion-neutral collision frequency (ν_{in}) suppressed EPB development via the suppression of RTI growth rate (γ).
2. High Hall conductivity (σ_H) during the storm event may have inhibited EPB development via reducing Pedersen current and subsequently, eastward polarization $\vec{E}$.
3. Ion-neutral collision frequency (ν_{in}) acts in consonance with Hall conductivity (σ_H) to reduce the growth rate of RTI (γ). We also believe that the high collision (ν_{in}) during this event may be a pointer that the burning of starlink satellites is associated with the high thermospheric neutral gas density.

References

[1] Akimasa Ieda. Ion-neutral collision frequencies for calculating ionospheric conductivity. 2020.

[2] Denny M Oliveira and Eftyhia Zesta. Satellite orbital drag during magnetic storms. *Space Weather*, 2019.

[3] Eurico R de Paula. et al. Ionospheric irregularity behavior during the september 6–10, 2017 magnetic storm over brazilian equatorial–low latitudes. 2019.

[4] Tatsuhiro Yokoyama. A review on the numerical simulation of equatorial plasma bubbles toward scintillation evaluation and forecasting. *Progress in Earth and Planetary Science*, 2017.

Future Research

For complete understanding of the thermosphere-ionosphere interaction during moderate storm event such as this, we intend to study:

- The influence of collision frequency on the integrated Pedersen and Hall Conductivity for selected (different) geomagnetic conditions including this event.
- The temporal variation in Rayleigh-Taylor Instability with collision frequency under different geomagnetic conditions including this event.
- Computing the exact magnitude and direction of equatorial Electric field during this storm event.

Acknowledgement

CNPq
NCAR UCAR
GOLD
IBGE

EMAIL: brians.amadi@inpe.br